Dipole radiation in a one-dimensional photonic crystal. II. TM polarization

Jorge R. Zurita-Sánchez* and Adán S. Sánchez
Instituto Nacional de Astrofísica, Óptica y Electrónica, Apartado Postal 51, Puebla, Puebla 72000, Mexico

P. Halevi†
Instituto Nacional de Astrofísica, Óptica y Electrónica, Apartado Postal 51, Puebla, Puebla 72000, Mexico and Department of Chemical Physics, The Weizmann Institute of Science, Rehovot 76100, Israel

(Received 7 June 2001; revised manuscript received 15 May 2002; published 21 October 2002)

As in a recent paper [I. Alvarado-Rodríguez, P. Halevi, and Adán S. Sánchez, Phys. Rev. E **63**, 056613 (2001); **65**, 039901(E) (2002)], we study the power emitted by an oscillating dipole in a superlattice (SL) modeled by means of a periodic distribution of Dirac-delta functions (*Dirac-comb* SL). However, while in the aforementioned paper the radiation was restricted to the transverse electric (TE) polarization mode, here we focus our attention on the transverse magnetic (TM) mode. Employing the same methodology, again we find that the power spectra are dominated by slope discontinuities. These occur — if at all — at the band edges for on-axis propagation, depending on the dipole's position and orientation. The largest enhancement or inhibition is present for normalized frequencies such that $(\omega d/c) \lesssim 2\pi$; here, ω is the dipole frequency, c is the speed of light in vacuum, and d is the distance between the barriers. For substantial values of the *grating strength* considerable enhancement or suppression of the radiated power (in comparison to the free-space value) is obtained. We also find that the power emitted by a gas of randomly oriented dipoles exhibits slope discontinuities at all band edges for on-axis propagation. In comparison with the TE polarization case, the TM polarization exhibits several different qualitative features.

DOI: 10.1103/PhysRevE.66.046613 PACS number(s): 42.70.Qs, 42.50.Gy

I. INTRODUCTION

This paper is a sequel to the preceding one by Alvarado-Rodríguez, Halevi, and Sánchez [1]. They both deal with the radiation emitted by a dipole embedded within a model superlattice (SL); the first paper (denoted by I) dealing with the transverse electric (TE) polarization component, while the present paper is dedicated to the transverse magnetic (TM) polarization contribution. A detailed introduction and an extensive list of references is given in I, so here we will limit ourselves to only the most essential.

In I, the theory of power emission in a linear inhomogeneous medium was summarized. This theory is a classical adaptation, developed by Dowling and Bowden [2], of the quantum electrodynamical theory (in the Weisskopf-Wigner approximation) of Glauber and Lewenstein [3]. The steady-state ($t=\infty$) power radiated by a point electric dipole, oscillating harmonically with frequency ω_o, is [2]

$$P=\pi^2\omega_o^2\mu^2\int d^3k\,|\mathbf{a}_{\mathbf{k}}(\mathbf{r}_0)\cdot\hat{\boldsymbol{\mu}}|^2\delta(\omega_o-\omega_{\mathbf{k}}). \tag{1}$$

Here, $\boldsymbol{\mu}=\mu\hat{\boldsymbol{\mu}}$ is the dipole momentum, $\mathbf{r}_0$ is the dipole position, and $\mathbf{a}_{\mathbf{k}}(\mathbf{r})$ are the vector potential eigenvectors. Notice that only those normal modes contribute to the radiated energy that have their eigenvalue $\omega_{\mathbf{k}}$ equal to ω_o and provided that the eigenvector $\mathbf{a}_{\mathbf{k}}(\mathbf{r}_o)$ is *not* perpendicular to the dipole momentum $\boldsymbol{\mu}$. Equation (1) applies to either polarization, and will be employed here to calculate the TM contribution.

The following section recapitulates the normal modes of the *Dirac-comb* SL, studied in detail in Ref. [4] for TM polarization. These modes are normalized in Sec. III, and the emitted power is calculated in Sec. IV. The results for the two fundamental configurations—with the dipole being parallel and perpendicular to the SL interfaces—are discussed in Secs. V and VI, respectively. The case of radiation by a gas of randomly distributed and oriented dipoles is addressed in Sec. VII. The paper is brought to conclusion in Sec. VIII.

II. NORMAL MODES

In Refs. [1,2,4,5], the *Dirac-comb* model is used to represent the dielectric SL, namely,

$$\epsilon(x)=\epsilon_0+gd\sum_{n=-\infty}^{\infty}\delta(x-nd). \tag{2}$$

Here, the g parameter is called the *grating strength*, d is the period of the SL, and ϵ_0 is the dielectric constant of the medium between the barriers.

The magnetic induction field $\mathbf{B}(\mathbf{r})$ lies in the yz plane for the TM modes. In Ref. [4], we expressed the magnetic induction in the nth region between the delta-function barriers, as

$$\mathbf{B}_{\mathbf{k}}^{(n)}(\mathbf{r})=B_{\mathbf{k}}^{(n)}(x)e^{i(k_y y+k_z z)}\hat{\mathbf{e}}_{\mathbf{k}}. \tag{3}$$

*Present address: The Institute of Optics, University of Rochester, Rochester, NY 14627.
†Electronic address: halevi@inaoep.mx

Here, $\hat{\mathbf{e}}_{\mathbf{k}}$ is a unit vector in the yz plane, perpendicular to the in-plane wave-vector $\mathbf{k}_{\parallel}$, which forms an angle ϕ with the z axis. It is defined as $\hat{\mathbf{e}}_{\mathbf{k}} = -\cos\phi\hat{\mathbf{y}} + \sin\phi\hat{\mathbf{z}}$, and $\mathbf{B}_{\mathbf{k}}^{(n)}(x)$ is given by

$$B_{\mathbf{k}}^{(n)}(x) = e^{ink_B d}[A_0 e^{iK(x-nd)} + B_0 e^{-iK(x-nd)}],$$

$$(n-1)d < x < nd, \quad n = 0, \pm 1, \pm 2 \ldots, \tag{4}$$

$$K = \sqrt{\frac{\omega^2}{c^2}\epsilon_0 - k_{\parallel}^2}, \tag{5}$$

where k_B is the Bloch wave vector and $k_{\parallel}$ is the magnitude of the projection of the wave-vector $\mathbf{k}$ on the yz plane, i.e., $k_{\parallel}^2 = k_y^2 + k_z^2$. Solving the eigenvalue problem for the Dirac-comb model, we obtained that the coefficients A_0 and B_0 of Eq. (4) are related by [4]

$$B_0 = \frac{e^{-ik_B d} - e^{-iKd}(1 - i\alpha)}{-i\alpha e^{iKd}} A_0. \tag{6}$$

Also, the dispersion relation was found to be

$$\cos k_B d = \cos Kd - \alpha(K)\sin Kd, \tag{7}$$

$$\alpha(K) = \frac{gd}{2\epsilon_0}K. \tag{8}$$

Equation (7) is an implicit equation for the frequency $\omega_{\mathbf{k}} = \omega(k_B, k_{\parallel})$. Equations (6) and (7) specify the normal modes of the magnetic induction field. It is important to notice that propagating solutions for the TM modes, that is, when k_B is real, occur only if K is real, too (unlike the TE modes, for which K may be imaginary).

III. MODE NORMALIZATION

In this section, a real superlattice (each cell composed of two layers $j = 1,2$ with dielectric constants ϵ_j and widths h_j) is first treated. Then, in Eqs. (4) and (5) A_0, B_0, K, and ϵ_0 must be replaced by A_j, B_j, K_j, and ϵ_j, respectively.

The set $\mathbf{a}_{\mathbf{k}}(\mathbf{r})$ must satisfy the following orthonormalization condition:

$$\int d^3 r \epsilon(\mathbf{r}) \mathbf{a}_{\mathbf{k}'}^*(\mathbf{r}) \cdot \mathbf{a}_{\mathbf{k}}(\mathbf{r}) = \delta(\mathbf{k} - \mathbf{k}'). \tag{9}$$

The vector potential $\mathbf{a}_{\mathbf{k}}(\mathbf{r})$ is related with magnetic induction $\mathbf{B}_{\mathbf{k}}(\mathbf{r})$ by

$$\mathbf{a}_{\mathbf{k}}(\mathbf{r}) = \frac{c^2}{\epsilon(\mathbf{r})\omega^2}\nabla \times \mathbf{B}_{\mathbf{k}}(\mathbf{r}). \tag{10}$$

In the 0th cell, substituting Eq. (3) in Eq. (10), we obtain

$$\mathbf{a}_{\mathbf{k}}^{(j)}(\mathbf{r}) = e^{i(k_y y + k_z z)}[a_{\mathbf{k}x}^{(j)}(x)\hat{\mathbf{x}} + a_{\mathbf{k}T}^{(j)}(x)(\sin\phi\hat{\mathbf{y}} + \cos\phi\hat{\mathbf{z}})], \tag{11}$$

where

$$j = \begin{cases} 1, & -d < x < -h_2, \\ 2, & -h_2 < x < 0, \end{cases}$$

and we have defined

$$a_{\mathbf{k}x}^{(j)}(x) = \frac{c^2}{\epsilon_j \omega^2} ik_{\parallel}[A_j e^{iK_j x} + B_j e^{-iK_j x}], \tag{12}$$

$$a_{\mathbf{k}T}^{(j)}(x) = -\frac{c^2}{\epsilon_j \omega^2} iK_j[A_j e^{iK_j x} - B_j e^{-iK_j x}]. \tag{13}$$

By the Bloch theorem, the normalization condition can be set to involve only the field in the cell $n = 0$, namely, $-d < x < 0$, that is,

$$\sum_{n=-\infty}^{\infty} e^{in(k_B - k_B')d}\left[\int_{-\infty}^{\infty} dy \int_{-\infty}^{\infty} dz \int_{-d}^{-h_2} dx \;\; \epsilon_1 \mathbf{a}_{\mathbf{k}'}^{(1)*} \cdot \mathbf{a}_{\mathbf{k}}^{(1)} + \int_{-\infty}^{\infty} dy \int_{-\infty}^{\infty} dz \int_{-h_2}^{0} dx \;\; \epsilon_2 \mathbf{a}_{\mathbf{k}'}^{(2)*} \cdot \mathbf{a}_{\mathbf{k}}^{(2)}\right] = \delta(\mathbf{k} - \mathbf{k}'). \tag{14}$$

Substituting Eq. (11) into Eq. (14) and using the facts that

$$\int_{-\infty}^{\infty} dy \int_{-\infty}^{\infty} dz e^{i[(k_y - k_y')y + (k_z - k_z')z]} = (2\pi)^2 \delta(k_y - k_y')\delta(k_z - k_z'),$$

$$d\sum_{n=-\infty}^{\infty} e^{in(k_B - k_B')d} = 2\pi\delta(k_B - k_B'),$$

the δ functions cancel out and Eq. (14) simplifies to

$$\epsilon_1 \int_{-d}^{-h_2} dx (a_{\mathbf{k}x}^{*(1)}(x) a_{\mathbf{k}x}^{(1)}(x) + a_{\mathbf{k}T}^{*(1)}(x) a_{\mathbf{k}T}^{(1)}(x)) + \epsilon_2 \int_{-h_2}^{0} dx (a_{\mathbf{k}x}^{*(2)}(x) a_{\mathbf{k}x}^{(2)}(x) + a_{\mathbf{k}T}^{*(2)}(x) a_{\mathbf{k}T}^{(2)}(x)) = \frac{d}{(2\pi)^3}. \tag{15}$$

Substituting Eqs. (12) and (13) into Eq. (15) and integrating we get

$$\frac{1}{\epsilon_1}\left\{\frac{\omega^2}{c^2}\epsilon_1(d-h_2)(|A_1|^2+|B_1|^2) + 2(k_\parallel^2-K_1^2)\mathrm{Re}\left[A_1B_1^*\frac{e^{-2iK_1h_2}-e^{-2iK_1d}}{2iK_1}\right]\right\} + \frac{1}{\epsilon_2}\left\{\frac{\omega^2}{c^2}\epsilon_2h_2(|A_2|^2+|B_2|^2) + 2(k_\parallel^2-K_2^2)\mathrm{Re}\left[A_2B_2^*\frac{1-e^{-2iK_2h_2}}{2iK_2}\right]\right\} = \frac{\omega^4 d}{(2\pi)^3c^4}. \tag{16}$$

Applying the δ limit $\epsilon_2h_2\to gd$ to the last equation and dropping the index "1" we get

$$\frac{K^2}{\epsilon}g|A-B|^2+\frac{\omega^2}{c^2}\epsilon(|A|^2+|B|^2) + 2(k_\parallel^2-K^2)\mathrm{Re}\left[AB^*\frac{1-e^{-2iKd}}{2iKd}\right] = \frac{\omega^4\epsilon}{(2\pi)^3c^4}. \tag{17}$$

Then, using Eq. (6), after considerable algebra, Eq. (17) is reduced to

$$|A|^2=\frac{\omega^2}{16\pi^3c^2}\frac{\sin Kd+\alpha\cos Kd+\sin k_Bd}{\left(1+\frac{2gK^2c^2}{\epsilon^2\omega^2}-\frac{\alpha}{Kd}\right)\sin Kd+\left(1+\frac{2gK^2c^2}{\epsilon^2\omega^2}\right)\alpha\cos Kd}. \tag{18}$$

IV. TM EMITTED POWER

We consider that the medium between the barriers is vacuum, and then the field that interacts with the dipole is given by Eq. (11) with $j=1$ and $\epsilon_1=1$. [For a dielectric medium ($\epsilon_1>1$) Eq. (11) is *not* valid, since one has to use the *local field*]. Then we can drop the layer index $j=1$. Also, without losing any generality, we suppose that the dipole position is

$$\mathbf{r}_0=x_0\hat{\mathbf{x}}+y_0\hat{\mathbf{y}}+z_0\hat{\mathbf{z}}, \quad -d<x_0<0, \tag{19}$$

and that it is parallel to the xy plane, with its orientation represented by

$$\hat{\boldsymbol{\mu}}=\sin\psi\hat{\mathbf{x}}+\cos\psi\hat{\mathbf{y}}. \tag{20}$$

Now, let us define the volume differential in $\mathbf{k}$ space as in Fig. 4 of Ref. [5],

$$d^3k=k_\parallel d\phi d\kappa_t d\kappa_n. \tag{21}$$

Here, $d\kappa_t$ and $d\kappa_n$ are the differential tangential and normal segments of the equifrequency surface. They can be expressed as

$$d\kappa_n=\frac{d\omega_{\mathbf{k}}}{|\nabla_{\mathbf{k}}\omega|}, \tag{22}$$

$$d\kappa_t=\sqrt{1+\left(\left.\frac{\partial k_B}{\partial k_\parallel}\right|_\omega\right)^2}\,dk_\parallel. \tag{23}$$

We calculate $|\nabla_{\mathbf{k}}\omega|$ and $\partial k_B/\partial k_\parallel$ from Eq. (7), and then Eq. (21) is found to be

$$d^3k=\frac{\omega|F|}{c^2|K\sin k_Bd|}k_\parallel dk_\parallel d\phi d\omega, \tag{24}$$

$$F\equiv\left[1+\frac{g}{2}\right]\sin Kd+\alpha\cos Kd. \tag{25}$$

Substituting Eq. (24) into Eq. (1) and integrating with respect to ω then gives

$$P=\frac{\pi^2\omega_0^3\mu^2}{c^2}\int d\phi dk_\parallel\ k_\parallel\left|\mathbf{a}_{\mathbf{k}}(\mathbf{r}_0)\cdot\hat{\boldsymbol{\mu}}\right|^2\left.\frac{|F|}{|K\sin k_Bd|}\right|_{\omega_0}. \tag{26}$$

Next, we substitute Eqs. (11), (19), and (20) into Eq. (26) and then integrate with respect to ϕ. This results in

$$P=\frac{2\pi^3c^2\mu^2}{\omega_0}\int dk_\parallel\ \ k_\parallel\frac{|F|}{|K\sin k_Bd|}I(\psi)(|A|^2+|B|^2) +J(\psi)2\mathrm{Re}(AB^*e^{2iKx_0}), \tag{27}$$

$$I(\psi)\equiv k_\parallel^2\sin^2\psi+\frac{1}{2}K^2\cos^2\psi, \tag{28}$$

$$J(\psi)\equiv k_\parallel^2\sin^2\psi-\frac{1}{2}K^2\cos^2\psi. \tag{29}$$

Then, using Eqs. (18) and (6), Eq. (27) becomes

$$P=\frac{\mu^2\omega_0}{4}\int dk_\parallel\ \ k_\parallel\frac{|F|}{|K\sin k_Bd|}\frac{I(\psi)(\sin Kd+\alpha\cos Kd)-J(\psi)\alpha\cos K(d+2x_0)}{\left(1-\frac{\alpha}{Kd}+\frac{2K^2c^2g}{\omega_0^2}\right)\sin Kd+\left(1+\frac{2K^2c^2g}{\omega_0^2}\right)\alpha\cos Kd}. \tag{30}$$

This is the final result for the power emitted by the electric dipole. The integration is carried out in terms of a single variable $k_\parallel$ for values of k_B that lie on the equifrequency surface ω_0. There is contribution to the emitted power only in those regions of $k_\parallel$ where k_B is real (in Ref. [4], we have plotted several equifrequency surfaces). There are two important orientations of the dipole: when it is parallel to the ''barriers'' ($\psi=0$) and when it is perpendicular to the ''barriers'' ($\psi=\pi/2$). The power emitted for any other orientation of the dipole can be represented as a linear combination of the powers emitted for these two basic orientations, that is

$$P(\omega_0,\psi)=\cos^2\psi P(\omega_0,\psi=0)+\sin^2\psi P(\omega_0,\psi=\pi/2). \tag{31}$$

It is convenient to work with the normalized dipole position $x_0/d=\xi_0$, the normalized frequency $\omega d/c=\Omega$, the normalized components of the wave vector: $k_Bd=\kappa_B$, $Kd=\kappa$, $k_\parallel d=\kappa_\parallel$, and the power normalized to the power emitted by a dipole in free-space $P_N=(3c^3/\omega_0^4\mu^2)P$. Using this normalization scheme in Eq. (30), we have

$$P_N(\Omega_0,0)=\frac{3}{8\Omega_0^3}\int d\kappa_\parallel\frac{\kappa_\parallel|F|}{|\kappa\sin\kappa_B|}\times\kappa^2\frac{\sin\kappa+\alpha\cos\kappa+\alpha\cos\kappa(1+2\xi_0)}{\left(1+\frac{2\kappa^2g}{\Omega^2}-\frac{\alpha}{\kappa}\right)\sin\kappa+\left(1+\frac{2\kappa^2g}{\Omega^2}\right)\alpha\cos\kappa}, \tag{32}$$

$$P_N(\Omega_0,\pi/2)=\frac{3}{4\Omega_0^3}\int d\kappa_\parallel\frac{\kappa_\parallel|F|}{|\kappa\sin\kappa_B|}\times\kappa_\parallel^2\frac{\sin\kappa+\alpha\cos\kappa-\alpha\cos\kappa(1+2\xi_0)}{\left(1+\frac{2\kappa^2g}{\Omega^2}-\frac{\alpha}{\kappa}\right)\sin\kappa+\left(1+\frac{2\kappa^2g}{\Omega^2}\right)\alpha\cos\kappa}. \tag{33}$$

$$F=(1+g/2)\sin\kappa+\alpha\cos\kappa, \tag{34}$$

$$\alpha=g\kappa/2. \tag{35}$$

V. DIPOLE PARALLEL TO "BARRIERS" ($\psi=0$)

In this section, we compute the normalized power as given by Eq. (32). The power emitted by the dipole as a function of the frequency is continuous, but it presents slope discontinuities (see Fig. 1). We can notice that such singularities occur for frequencies coinciding with a band edge at $k_\parallel=0$ (on-axis propagation), since the group velocity for such $\mathbf{k}$ is zero ($\nabla_{\mathbf{k}}\omega=\mathbf{0}$), see Eq. (23) of Ref. [4]. These are known as van Hove singularities or as analytical critical points. As can be expected, the slope discontinuities are much more pronounced for the larger value of the grating strength ($g=0.9$). Nevertheless, for certain band-edge frequencies at $k_\parallel=0$ the slope discontinuities are missing. Mathematically, the van Hove singularities are associated with $\kappa_\parallel$ and $\sin\kappa_B$ both vanishing in the last factor of Eq. (32), namely, a singularity of the 0/0 type.

In order to gain some understanding of the role of the dipole-field interaction, now we analyze the case when the numerator of Eq. (32) vanishes. For on-axis propagation

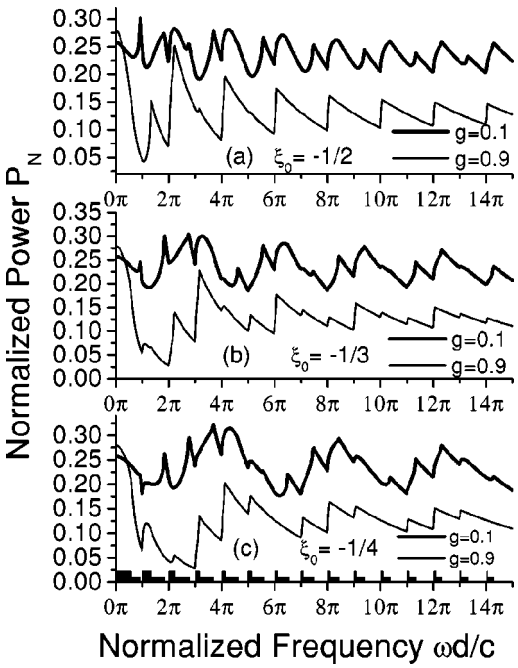

FIG. 1. Normalized power emitted by a dipole oriented parallel to the barriers as a function of the normalized frequency $\omega d/c$ for $g=0.1$ and $g=0.9$ and three dipole positions. The width of the lower (upper) box on the frequency axis indicates the extensions of the allowed bands for $g=0.1$ ($g=0.9$). (a) For $\xi=-1/2$ there are *no* slope discontinuities at $\omega d/c=\pi(2m+1)$, $m=1,2\ldots$. (b) For $\xi=-1/3$ there are slope discontinuities at $\omega d/c=m\pi$, $m=1,2\ldots$. (c) $\xi=-1/4$, there are *no* slope discontinuities at $\omega d/c=2\pi(2m+1)$, $m=0,1,2\ldots$.

($\kappa_{\|}=0$, $\kappa=\Omega$, where we drop the subscript ''0'' henceforth), this occurs when

$$\frac{\sin\Omega}{g\Omega}=-\frac{1}{2}\{\cos\Omega+\cos[\Omega(1+2\xi)]\}. \tag{36}$$

In Ref. [4], it was shown that the lower band edges for on-axis propagation are defined by $\Omega=\omega d/c=\pi n$, where $n=(0,1,2,\ldots)$ is the band index, and are thus independent of g. For such band-edge frequencies $\sin\Omega=0$, so the condition (36) reduces to

$$\cos(n\pi\xi)=0. \tag{37}$$

This factor can be traced to the transverse part of $\mathbf{a}_{\mathbf{k}}(\mathbf{r}_0)$, Eq. (13) (the longitudinal part vanishes for $k_{\|}=0$). Because, under the conditions considered $A=-B$, we see that $a_{\mathbf{k}T}(x_0)$ is proportional to $\cos(n\pi\xi)$. Now, in the Coulomb gauge that we are employing, the electric field is $\mathbf{E}(\mathbf{r})=i(\omega/c)\mathbf{a}(\mathbf{r})$ [1]; hence, the factor (37) corresponds to the electric field squared in the dipole field interaction $|\mathbf{a}_{\mathbf{k}}(\mathbf{r}_0)\cdot\hat{\boldsymbol{\mu}}|^2$ in Eq. (1). When this factor vanishes, the dipole cannot interact with the field, and then the contribution of the mode $k_{\|}=0$ to the emitted power is zero. As a consequence, the aforementioned slope discontinuities in $P(\omega)$ do *not* arise at the lower band edges for on-axis propagation. The expression (37) vanishes if $|\xi|=(2m+1)/(2n)$, where $m=0,1,2,\ldots$, that is, *when the dipole position is given by the ratio of an odd and an even number* $|\xi|<1$. For a given ξ, this corresponds to the normalized frequencies $\Omega=\pi n=\pi(m+1/2)/|\xi|$, with the understanding that $(m+1/2)/|\xi|$ is integer. For example, if the dipole is located midway between two barriers, $\xi=-1/2$, we have $\Omega=\pi(2m+1)$; in Fig. 1(a), the slope discontinuities are indeed absent for $\Omega=\pi,3\pi,5\pi,7\pi,\ldots,$. In the case of $\xi=-1/3$, the factor (37) does *not* vanishes for any m, and then the discontinuities are present [see Fig. 1(b)]. By using the same relation, for $\xi=-1/4$ the discontinuities are absent when $\Omega=2\pi,6\pi,10\pi,\ldots$, as we can notice in Fig. 1(c). The absence of the aforementioned discontinuities is responsible for the distinctive repetitive patterns that can be seen in Figs. 1(a), 1(b), and 1(c). This behavior is a consequence of the electric field having a node at the dipole position for certain modes. Then the plots shown in Fig. 1 follow a quasi periodic pattern whose shape is determined by the dipole position.

In the limit $g\to 0$, Eq. (32) can be easily integrated, resulting that the normalized power is a constant equal to 1/4. In this limit, the SL is reduced to free space and we see that the TM modes contribute 1/4 of the radiated power. Obviously, the rest of the normalized power, that is 3/4, is contributed by the TE modes. This, indeed, has been found in I for $\psi=0$. We then define the ''enhancement'' as $(P_N-0.25)/0.25=4P_N-1$, obviously for $P_N>0.25$. If, on the other hand, $P_N<0.25$ then there is a ''reduction'' $1-4P_N$.

The enhancement of the normalized power is moderate for both values of g. In Fig. 1, for $g=0.1$, the largest enhancement is an increase of about 25% with respect to free space and is attained at the frequencies that correspond to the band edges. For $g=0.9$, the maximum enhancement is an increase of just 10% at $\omega=0$. The maximum reductions obtained are 85 and 30 % of the free space value 1/4 for $g=0.9$ and $g=0.1$, respectively.

It can be proved that, in the limit of low frequencies, $\omega\to 0$, the normalized power is a constant that depends only on the g parameter, given by

$$P_N(0,0)=\frac{3(1+g)^{3/2}}{4(2g+g^2)}\left(1-\frac{1}{\sqrt{2g+g^2}}\arctan\sqrt{2g+g^2}\right). \tag{38}$$

In this long-wavelength limit, the power obviously cannot depend on the dipole's position, the SL becoming an effectively homogeneous medium. To obtain the above equation, we use the fact that $\kappa\ll 1$; thus, the following approximations can be done in Eq. (32): $\cos\kappa\approx 1$, $\sin\kappa\approx\kappa$, $\cos\kappa(1+2\xi)\approx 1$, $F\approx(1+g)\kappa$, and $\sin\kappa_B\approx\sqrt{1+g}\,\kappa$. The ensuing definite integral, containing only g as a parameter, can be solved. As a result, Eq. (38) is obtained. The normalized power as a function of the grating strength g increases until it reaches its maximum value $P_N\approx 0.28$ at $g\approx 1.172$. This is a small enhancement with respect to free-space value 0.25. For $g>1.172$, the normalized power decreases, and it tends to zero as $g\to\infty$. We have computed Eq. (38) for $g=0.9$ and for $g=0.1$, resulting in 0.279 and 0.257, respectively, for the normalized power. These results are in agreement with the values shown in Fig. 1.

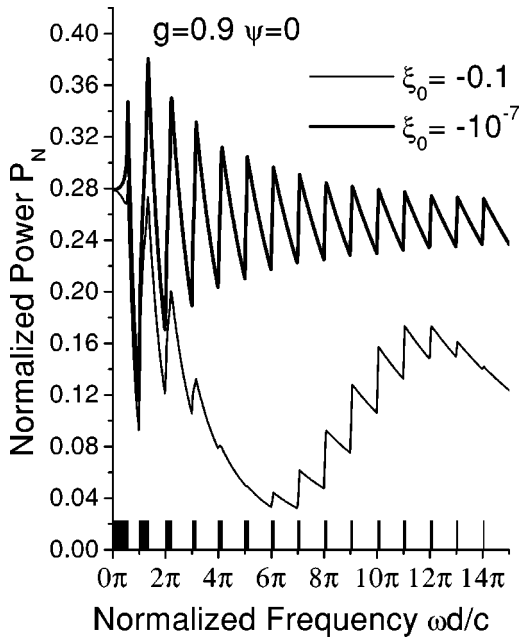

FIG. 2. Normalized power emitted by a dipole located close to one of the barriers ($\xi_o=-0.1$ and $\xi_o=-10^{-7}$) as a function of the normalized frequency $\omega d/c$ for $g=0.9$. The dipole is oriented parallel to the barriers ($\psi=0$). The width of box on the frequency axis indicates the extension of the allowed bands for $g=0.9$.

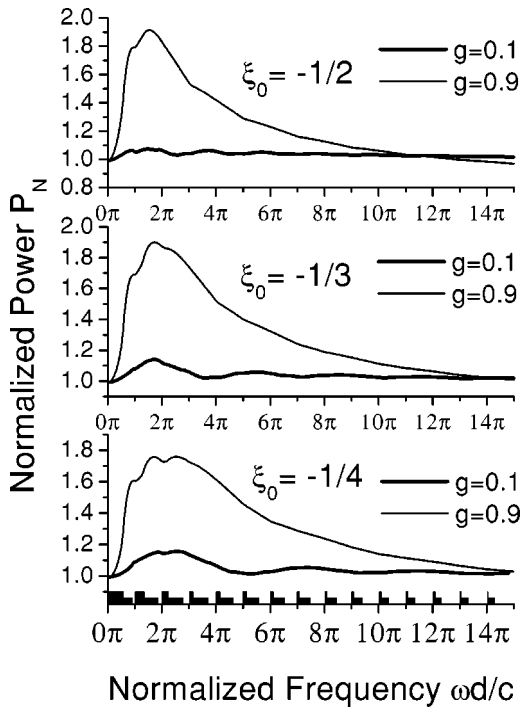

FIG. 3. Normalized power emitted by a dipole oriented perpendicular to the barriers as a function of the normalized frequency $\omega d/c$ for $g=0.1$ and $g=0.9$ and three dipole positions. The width of the lower (upper) box on the frequency axis indicates the extension of the allowed bands for $g=0.1$ ($g=0.9$).

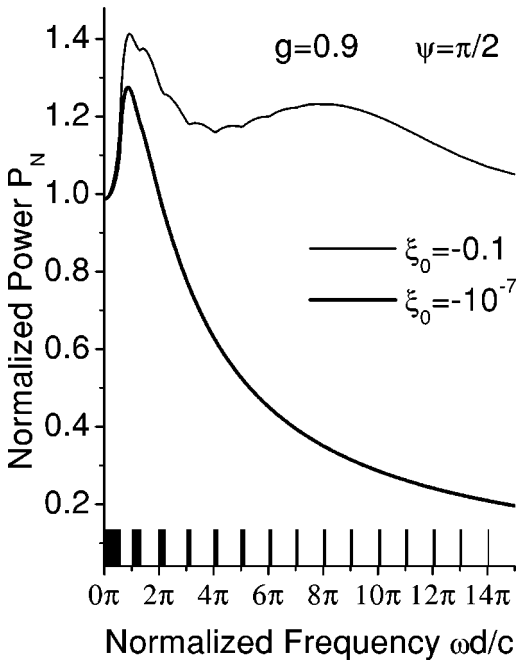

FIG. 4. As Fig. 2; however, with the dipole oriented perpendicular to the barriers ($\psi=\pi/2$).

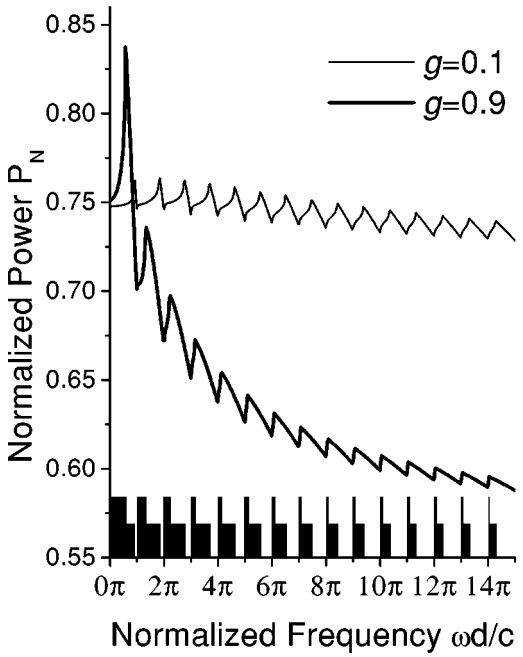

FIG. 5. The normalized average power per dipole versus the normalized frequency ($\omega d/c$) for $g=0.1$ and $g=0.9$. The width of the lower (upper) box on the frequency axis indicates the extension of the allowed bands for $g=0.1$ ($g=0.9$). The power radiated by the gas of dipoles is obtained by multiplying by the number of dipoles. We have slope discontinuities at all the frequencies that correspond to the band-gap edges (for on-axis propagation).

As the dipole approaches one of the barriers, there is a further enhancement (up to 50%) of the normalized emitted power; however, this enhancement is not related to the resonant effect found for the TE modes (see Fig. 3 of I). This is shown in Fig. 2 for the dipole positions $\xi=-0.1$ and $\xi=-10^{-7}$ with $g=0.9$. This difference of behavior can be explained by comparing the dispersion relations of the TE and the TM modes. In the case of TE polarization, the propagation modes can exhibit evanescent behavior just outside the barriers, which gives rise to the enhancement. On the other hand, for TM polarization, such evanescent modes are *not* allowed for the Dirac-comb model.

VI. DIPOLE PERPENDICULAR TO "BARRIERS" $\psi=\pi/2$

Computing Eq. (33), we find that the function $P_N(\omega)$, (as for $\psi=0$) is continuous, but it presents slope discontinuities (see Fig. 3). The normalized power is strongly modified for not very large frequencies ($\Omega<\sim 5\pi$). We can see from Fig. 3 that, in this range, as g increases, the power is enhanced considerably. We recall from I that a perpendicular dipole cannot emit TE radiation. Therefore, the enhancement relative to free space is simply P_N-1 (for $P_N>1$). For $g=0.9$, the greatest enhancement is about 90% for $\xi=-1/2$ and $\xi=-1/3$, and about 80% for $\xi=-1/4$. On the other hand, for $g=0.1$, the maximum enhancement is around 10%. The normalized power for greater frequencies ($\Omega\geqslant 5\pi$) fluctuates around 1.00.

In Sec. V, for $\psi=0$, we saw that some of the slope discontinuities arise at the band edges for on-axis propagation. For $\psi=\pi/2$, the slope discontinuities in the power spectrum are still present, however, they are very weak. This can be understood from the fact that, for this dipole orientation, the dipole cannot couple to the field modes for on-axis propagation. This is so because $\mathbf{a_k}(\mathbf{r}_0)$ is perpendicular to the SL axis for $k_\parallel=0$ [see Eq. (12)]. Mathematically, this is revealed by the factor $k_\parallel$ in Eq. (12), which weakens the singularities.

Equation (33) can be easily integrated in the limit $g\to 0$, with the result that the normalized power is equal to one. This was expected since, for this orientation of the dipole, there is no contribution to the power by the TE modes as commented above.

In the limit of low frequencies ($\omega\to 0$), the normalized power is again a constant independent of the dipole's position, namely,

$$P_N(0,\pi/2)=\frac{3\sqrt{1+g}}{2(2g+g^2)}\left(\frac{(1+g)^2}{\sqrt{2g+g^2}}\arctan\sqrt{2g+g^2}-1\right). \tag{39}$$

We obtain this equation by applying the same approximations described in the preceding section in Eq. (33). For $g=0.1$ and $g=0.9$, this formula for the normalized power gives 1.008 and 1.007, respectively. This is approximately in accord with the intercepts on the P_N axis in Fig. 3. The reason that the low-frequency result is different than Eq. (38) for the $\psi=0$ case, is that in this long-wavelength limit the SL behaves like a uniaxial crystal (with its optical axis parallel to the SL axis) having form birefringence.

In Fig. 4, the normalized emitted power is shown for $g=0.9$ and for the dipole's position close to the barrier ($\xi=-0.1$ and $\xi=-10^{-7}$). Here, we notice that the maximum enhancement actually decreases as the dipole approaches the barrier.

VII. DIPOLAR RADIATION BY A GAS

We consider a gas formed by a set of randomly oriented dipoles, which are also randomly distributed in the range $-d<x<0$, and do not interact among each other. We obtain the average, over ψ and ξ, of the power radiated by one dipole. The squared cosines and sines of ψ in Eqs. (28) and (29) have the spatial average of 1/3 and 2/3, respectively. The cosine function of Eq. (30), whose argument involves x_0, averages to $\sin(Kd)/Kd$. As a result, the average normalized power $\overline{P}_N(\Omega)$ per dipole is

$$\overline{P}_N(\Omega)=\frac{1}{8\Omega^3}\int d\kappa_\parallel\frac{\kappa_\parallel|F|}{|\kappa\sin\kappa_B|}\frac{(4\kappa_\parallel^2+\kappa^2)(\sin\kappa+\alpha\cos\kappa)-\alpha(4\kappa_\parallel^2+\kappa^2)\sin\kappa/\kappa}{\left(1+\frac{2\kappa^2 g}{\Omega^2}-\frac{\alpha}{\kappa}\right)\sin\kappa+\left(1+\frac{2\kappa^2 g}{\Omega^2}\right)\alpha\cos\kappa}. \tag{40}$$

In Fig. 5, we plot the total average power radiated per dipole versus the normalized frequency ($\omega d/c$) of oscillation. The total power radiated by the gas is obtained simply by multiplying by the number of dipoles. Since there is no preferential orientation or localization of the dipoles, all the slope discontinuities are present at the frequencies that correspond to the band edges. The grating strength assumes the values $g=0.1$ and $g=0.9$.

VIII. CONCLUSION

We have presented the calculation of the power emitted by a dipole for several dipole positions, for the grating strengths $g=0.1$ and $g=0.9$, and for the two basic orientations of the dipole ($\psi=0,\pi/2$). We also presented the power emitted by a gas formed by randomly oriented and randomly distributed dipoles. We conclude that the effects of interest for controlling the power emitted by a dipole occur at fre-

quencies that correspond to the band-gap edges (for on-axis propagation), since there the field-dipole interaction is strongly modified. Roughly speaking, the greatest enhancements or inhibitions of radiated power occur for relatively low frequencies, Ω is less than $\sim 5\pi$. When the dipole is parallel to the barriers, the effects caused by the SL on the radiation are more pronounced.

There is no remarkable power enhancement for dipole positions very close to a barrier, as was found for the TE polarization modes. This is true because, according to Eq. (7), K must be real, so quasiresonant excitation of evanescent modes is not possible as in I. Nevertheless, such absence of evanescent modes is a peculiarity of the Dirac-comb SL; these modes *are* present in a realistic description of the SL.

In the low-frequency limit, the power emitted is proportional to ω^4 as for free-space emission and it is independent of the dipole's position. However, it depends on the grating strength g and the dipole's orientation ψ. The latter feature is a manifestation of birefringence. The power emitted by a gas formed by dipoles is also strongly modified, presenting slope discontinuities at the band edges corresponding to on-axis propagation. The slope discontinuities of the density of states and almost all the slope discontinuities of $P(\omega)$ are located at frequencies corresponding to the band edges for on-axis propagation. Also, for fractional dipole positions certain discontinuities are absent.

The total emitted power is obtained by summing the TE [Eq. (32) of I] and the TM [Eq. (31)] contributions

$$\begin{aligned} P(\omega,\psi) &= P_{TE}(\omega,\psi) + P_{TM}(\omega,\psi) \\ &= [P_{TE}(\omega,0) + P_{TM}(\omega,0)]\cos^2\psi \\ &\quad + P_{TM}(\omega,\pi/2)\sin^2\psi. \end{aligned} \tag{41}$$

Therefore, if the dipole is perpendicular to the barriers ($\psi = \pi/2$), the emitted radiation is entirely TM polarized and the corresponding power is given by Eq. (33) and Figs. 3 or 4.On the other hand, for a dipole that is parallel to the barriers ($\psi = 0$), the total emitted power is given by the expression above in the square brackets, and it has both TE and TM components. Also, for a dipole gas the total power is obtained by adding the Figs. 4 of I and Fig. 5 of this paper.

ACKNOWLEDGMENTS

J.R.Z. and A.S.S. thank CONACyT and Sistema Nacional de Investigadores for financial support. P.H. is the recipient of CONACyT Grant No. 32191-E.

[1] I. Alvarado-Rodríguez, P. Halevi, and Adán S. Sánchez, Phys. Rev. E **63**, 56 613 (2001); **65**, 039901(E) (2002), denoted by I.
[2] J.P. Dowling and C.M. Bowden, Phys. Rev. A **46**, 612 (1992).
[3] Roy J. Glauber and M. Lewenstein, Phys. Rev. A **43**, 467 (1991).
[4] Jorge R. Zurita-Sánchez and P. Halevi, Phys. Rev. E **61**, 5802 (2000)
[5] I. Alvarado-Rodríguez, P. Halevi, and J.J. Sánchez-Mondragón, Phys. Rev. E **59**, 3624 (1999).